

See discussions, stats, and author profiles for this publication at: <https://www.researchgate.net/publication/221838825>

# Synthesis and biological validation of novel pyrazole derivatives with anticancer activity guided by 3D-QSAR analysis

ARTICLE *in* BIOORGANIC & MEDICINAL CHEMISTRY · MARCH 2012

Impact Factor: 2.79 · DOI: 10.1016/j.bmc.2012.01.032 · Source: PubMed

---

CITATIONS

24

---

READS

87

5 AUTHORS, INCLUDING:



**Karmen Brajša**

Galapagos Research Institute

29 PUBLICATIONS 284 CITATIONS

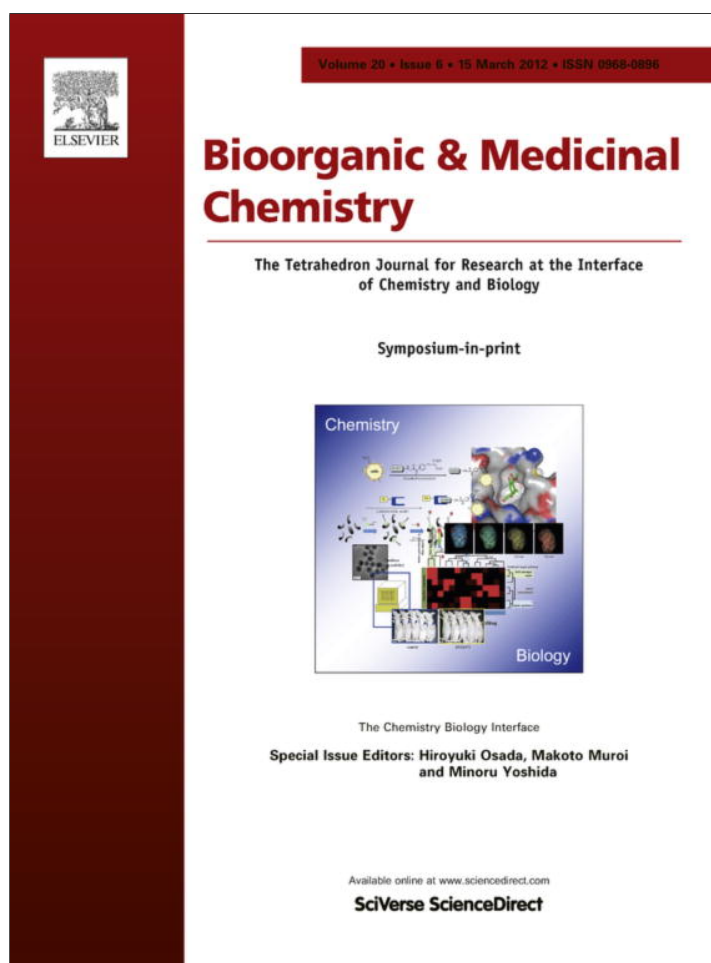
SEE PROFILE



**Branimir Bertosa**

20 PUBLICATIONS 227 CITATIONS

SEE PROFILE



This article appeared in a journal published by Elsevier. The attached copy is furnished to the author for internal non-commercial research and education use, including for instruction at the authors institution and sharing with colleagues.

Other uses, including reproduction and distribution, or selling or licensing copies, or posting to personal, institutional or third party websites are prohibited.

In most cases authors are permitted to post their version of the article (e.g. in Word or Tex form) to their personal website or institutional repository. Authors requiring further information regarding Elsevier's archiving and manuscript policies are encouraged to visit:

<http://www.elsevier.com/copyright>



Contents lists available at [SciVerse ScienceDirect](http://www.sciencedirect.com)

# Bioorganic & Medicinal Chemistry

journal homepage: [www.elsevier.com/locate/bmc](http://www.elsevier.com/locate/bmc)



## Synthesis and biological validation of novel pyrazole derivatives with anticancer activity guided by 3D-QSAR analysis

Ines Vujasinović<sup>a,†</sup>, Andrea Paravić-Radičević<sup>b,†</sup>, Kata Mlinarić-Majerski<sup>a</sup>, Karmen Brajša<sup>b,†</sup>, Branimir Bertoša<sup>c,\*</sup>

<sup>a</sup> Department of Organic Chemistry and Biochemistry, Ruđer Bošković Institute, Bijenička cesta 54, 10000 Zagreb, Croatia

<sup>b</sup> GlaxoSmithKline Research Centre Zagreb, Prilaz b. Filipovića 29, Zagreb, Croatia

<sup>c</sup> Department of Physical Chemistry, Ruđer Bošković Institute, Bijenička cesta 54, 10000 Zagreb, Croatia

### ARTICLE INFO

#### Article history:

Received 8 December 2011

Revised 18 January 2012

Accepted 19 January 2012

Available online 28 January 2012

#### Keywords:

QSAR

VolSurf+

Pyrazole

Amidooxime

Antitumor activity

A549 and NCIH23 lung cancer cells

### ABSTRACT

Using literature data on anticancer activity of pyrazole derivatives, 3D-QSAR models were developed and 3D-QSAR analysis was performed. The 3D-QSAR analysis enabled identification of molecular properties that have the highest impact on antitumor activity against lung cancer cells. The results of 3D-QSAR analysis were taken into account while new compounds were designed. Obtained 3D-QSAR models were used for prediction of activity of new compounds. In this way, design of new compounds was guided by 3D-QSAR analysis which was performed on literature data. Ten new pyrazole derivatives were synthesised and their antitumor activities against A549 and NCIH23 lung cancer cells were validated. In order to obtain full profile of anticancer activity, cells viability (MTS) assays were combined with cell proliferation (BrdU) assays which measure actively dividing cells in treated sample. Experimental measurements showed good agreement between predicted and measured activities for majority of compounds. Also, anticancer activities of new pyrazole derivatives pointed to the chemical groups that can be useful in designing antitumor molecules. Substitution of hydrazine linker with rigid, 1,2,4-oxadiazole moiety resulted in compound **10**, which has low (if any) cytotoxic activity and high potential cytostatic activity. Therefore, compound **10** presents a good starting point for design of new, more potent and safer anticancer therapeutics.

© 2012 Elsevier Ltd. All rights reserved.

### 1. Introduction

Lung cancer remains major global health problem,<sup>1</sup> accounting for more than a million annual deaths worldwide. It is the second most commonly occurring form of cancer in most Western countries and it is the leading cancer-related cause of death. In contrast to the mortality rate in men, which began declining more than 20 years ago, women's lung cancer mortality rates have been rising for over the last decades and are just recently beginning to stabilize.<sup>2</sup> Since current treatment modalities are inadequate, the discovery and development of new, more active, more selective and less toxic compounds for the treatment of malignancy are one of the most important goals in medicinal chemistry. In fact, cancer chemotherapy has entered a new era of molecularly targeted therapeutics, which is highly selective and not associated with the serious toxicities of conventional cytotoxic drugs.<sup>3</sup>

The pyrazole ring is a prominent structural motif found in numerous pharmaceutically active compounds. Due to the easy preparation and rich biological activity, pyrazole framework plays an essential role in biologically active compounds and therefore represents an interesting template for combinatorial<sup>4,5</sup> as well as medicinal chemistry.<sup>6–8</sup> Numerous representatives of this heterocycle exhibit anti-viral/antitumor,<sup>9,10</sup> antibacterial,<sup>11–13</sup> antiinflammatory,<sup>6</sup> analgesic,<sup>14</sup> fungistatic,<sup>15</sup> and anti-hyperglycemic activity.<sup>16,17</sup> Also, some arylpyrazoles were reported to have non-nucleoside HIV-1 reverse transcriptase inhibitory activity.<sup>18</sup> Extensive studies have been devoted to arylpyrazole derivatives such as Celecoxib, a well-known cyclooxygenase-2 inhibitor.<sup>19–21</sup>

Large amount of experimental data on anticancer activity of pyrazole derivatives can be useful in designing new compounds with anticancer activity. Computational chemistry tools can help in extracting the most useful information from large amount of experimental data and enable their usage in designing new compounds. Quantitative Structure–Activity Relationship (QSAR) studies have often been applied to find correlations between biological activities and molecular descriptors for different classes of compounds.<sup>22–24</sup> Such correlations can enable identification of the molecular properties which are the most important for biological

\* Corresponding author. Tel.: +385 1 456 10 25; fax: +385 1 468 02 45.

E-mail address: [bbertosa@irb.hr](mailto:bbertosa@irb.hr) (B. Bertoša).

† Present address: Galapagos Research Centre, Prilaz b. Filipovića 29, Zagreb, Croatia.

activity. In the same time, obtained models can be used for predicting activity of the compound whose activity has not been measured.

In the presented work, we have used VolSurf+ program to perform 3D-QSAR analysis on the series of pyrazole compounds<sup>25–30</sup> with measured antitumor activity towards A549 lung cancer cells. Up to our knowledge, this is the first attempt to use this dataset<sup>25–28</sup> for generating 3D-QSAR models in order to identify the most important molecular properties for the antitumor activity of pyrazole rings. VolSurf+ software has already been used for predicting antitumor activity of novel heterocyclic compounds and experiments proved its reliability.<sup>31</sup> The main advantages of the VolSurf+ based procedure are: (i) it does not depend on the alignment of the molecules and (ii) the molecular descriptors used in building QSAR model have clear physical or chemical meaning.<sup>32,33</sup> Results of 3D-QSAR analysis helped us to design new compounds, to predict their biological activities and to make a prioritization in synthesis. In this way, 3D-QSAR analysis served us as guideline in planning experiments.

Ten new pyrazole derivatives were synthesised and their antitumor activity against two lung cancer cell lines (A549 and NCIH23) were measured. Beside the A549 lung cancer cells (which were used for building 3D-QSAR models), activity of new compounds was also tested against NCIH23, human cell lines adenocarcinoma, that are commonly used in determination of antitumor activity of new chemical entities. Antitumor activity was characterized using cells viability (MTS) assays and cell proliferation (BrdU) assays. Cell viability indicates healthy cells in cell population and such assays cannot distinguish if the treated cells are in active phase of proliferation or not. Therefore, to have full profile of anticancer activity, cells viability assays should be combined with cell proliferation assays which measure actively dividing cells in treated sample. Using such approach, compound with low (if any) cytotoxic activity and high potential cytostatic activity was found.

## 2. Results and discussion

### 2.1. 3D-QSAR analysis

3D-QSAR analysis was performed on the 51 compounds whose antitumor activity against A549 lung cancer cells was described in the literature.<sup>25–28</sup> Two main goals of the performed 3D-QSAR analysis were: (1) identification of molecular properties that have the highest impact on antitumor activity against A549 cancer cells, (2) prediction of antitumor activity of new, yet unsynthesized, compounds. Using 3D-QSAR analysis, new compounds were designed and their antitumor activities were predicted. In this way, 3D-QSAR analysis served us as a guideline in choosing new candidates for synthesis and biological measurements. In the same time, the results of biological measurements of new compounds presented in this paper enabled validation of the 3D-QSAR approach.

#### 2.1.1. 3D-QSAR models

Several different 3D-QSAR models were built using the VolSurf+ program.<sup>32,33</sup> Detailed description of the procedure is given in Section 4. Models in which raw data were used and models in which completely inactive compounds were omitted were found to be more reliable than all other generated models (Table 1). The latter can be explained by the fact that in some cases lack of compound's activity is caused by insolubility, not by inadequate structural properties of the compound, and by the fact that the exact activity of inactive compounds was not given in the literature (Table S1 in Supplementary data).<sup>25–28</sup> Models 1 and 2 (Table 1, Fig. 1), both obtained using raw data, were shown to be the most trusted ones and were used for identification of the molecular descriptors that have

the highest impact on compound's activity. Model 2 actually constitutes external validation of model 1, dataset compounds were divided into the training set (used to build model) and test set (used for external prediction, compounds: **S5**, **S14**, **S21**, **S25**, **S29**, **S39**, **S44**, **S45**, **S46**, **S49** (Table S1 in Supplementary data)) using random number generator ([www.random.org](http://www.random.org)). Model 1 was also used for the prediction of the activity of new, yet unsynthesised compounds.

#### 2.1.2. Identification of the most important descriptors

Principal component analysis (PCA) was performed on the molecular descriptors of dataset compounds used for building model 1. The first two principal components (PCs) explained 84% of X-matrix variation. PCA loadings plot shows contribution of each descriptor to the first two PCs (Fig. 2). Since PCs are constructed in a way that the first few components describe majority of the X-matrix variance, their loadings describe descriptors with the highest contribution to the overall variance in the X-space PCs (which implies that their variation between the compounds is the most pronounced).

Following descriptors were identified as the ones with the highest variation between the compounds: W1–W3 (hydrophilic volumes), WN1 (weak H-bond interaction in which compound interacts as H-bond acceptor), WO1 (weak H-bond interaction in which compound interacts as H-bond donor), V (volume), D1 (hydrophobic regions), HSA (the sum of hydrophobic surface areas), S (surface) and MW (molecular mass).

The influence of each descriptor to the QSAR model can be estimated from its PLS coefficient, while the real impact of a descriptor on the biological activity is given as the product of the descriptor's value and its PLS coefficient. In order to investigate impact of each descriptor on the biological activity, product between average value of the descriptor (calculated for the dataset used to build the model) and its associated PLS coefficient was calculated for models 1 (Fig. 3) and 2 (Fig. S1 in the Supplementary data). In this way, following descriptors were found to have positive impact on antitumor activity against A549 cells: hydrophilic volumes which are descriptors related to polarizability and dispersion forces (W2, W3 W4), molecular volume (V), molecular mass (MW), hydrophobic interactions at energy level of  $-0.2$  kcal/mol (D1), the ability of the compound to make weak H-bond interaction with carbonyl group (WO1) and percentage of unionized species at pH 7 and 8 (%FU7, %FU8). The latter finding is in accordance with recently published investigation that identified presence of a protonable function as one of the major structural conditions for antitumor activity of 8-hydroxyquinoline substituted benzylamines.<sup>34</sup> Average values of some of positively correlated descriptors of the dataset compounds with the  $pIC_{50}$  values higher than 5.00 (compounds: **S41**, **S43**, **S45**, **S47–S51**) are:  $V=999.5 \text{ \AA}^3$ ,  $MW=455.0 \text{ g/mol}$ ,  $W2=896.4 \text{ kcal/mol}$ ,  $D1=396 \text{ kcal/mol}$ ,  $WO1=164.7 \text{ kcal/mol}$ , %FU7=96.5%, %FU8=73.2%. In case of the least active dataset compounds used for building model 1 (compounds with  $pIC_{50}$  lower than 4.20: **S1**, **S15**, **S17**, **S18**, **S21**, **S23**, **S35**), the average values of the same descriptors are:  $V=848.7 \text{ \AA}^3$ ,  $MW=376.4 \text{ g/mol}$ ,  $W2=898.5 \text{ kcal/mol}$ ,  $D1=255.9 \text{ kcal/mol}$ ,  $WO1=247.9 \text{ kcal/mol}$ , %FU7=99.9%, %FU8=99.7%. Interestingly, descriptor related to hydrophilic volume at the lowest energy value ( $-0.2$  kcal/mol) (W1) had negative impact on activity. Other descriptors with the highest negative correlation with antitumor activity against A549 cells are: ability of the compound to make weak H-bond interaction in which it interacts as H-bond acceptor (WN1), molecular surface (S) and percentage of unionized species at pH 10 (%FU10). The findings that %FU7 and %FU8 descriptors have positive, while %FU10 has negative correlation with activity indicate a weak acidic function as favorable for the antitumor activity of investigated compounds. Average values of some of neg-

**Table 1**  
Statistical properties of 3D-QSAR models

Model	nO <sup>a</sup>	nLV <sup>b</sup>	R <sup>2</sup>	SDEC <sup>c</sup>	Q <sup>2d</sup>	SDEP <sup>e</sup>	SDEP-ext <sup>f</sup>	nOE <sup>g</sup>	Scaling <sup>h</sup>
1 <sup>i</sup>	40	6	0.93	0.10	0.86 (0.81) <sup>j</sup>	0.15 (0.17) <sup>j</sup>			–
2 <sup>i</sup>	31	6	0.95	0.09	0.85 (0.81) <sup>j</sup>	0.16 (0.18) <sup>j</sup>	0.21	9	–
3	51	5	0.84	0.26	0.75 (0.77) <sup>j</sup>	0.32 (0.30) <sup>j</sup>			–
4	51	4	0.87	0.23	0.78 (0.75) <sup>j</sup>	0.30 (0.32) <sup>j</sup>			+
5 <sup>i</sup>	40	6	0.95	0.09	0.83 (0.75) <sup>j</sup>	0.16 (0.20) <sup>j</sup>			+
6 <sup>i</sup>	38	5	0.88	0.21	0.77 (0.74) <sup>j</sup>	0.30 (0.31) <sup>j</sup>	0.37	13	–
7 <sup>i</sup>	38	4	0.89	0.20	0.76 (0.68) <sup>j</sup>	0.30 (0.35) <sup>j</sup>	0.29	13	+
8 <sup>i</sup>	31	6	0.96	0.08	0.79 (0.73) <sup>j</sup>	0.18 (0.21) <sup>j</sup>	0.14	9	+
9 <sup>k</sup>	10	2	0.91	0.23	0.66 (0.64) <sup>j</sup>	0.44 (0.45) <sup>j</sup>	0.45	41	+

<sup>a</sup> Number of objects used to build the model (training set).

<sup>b</sup> Number of latent variables.

<sup>c</sup> SDEC is standard deviation of error of calculation.

<sup>d</sup> Q<sup>2</sup> is the cross-validated predictive performance.

<sup>e</sup> SDEP is the standard deviation in cross-validated prediction.

<sup>f</sup> SDEP for the external prediction.

<sup>g</sup> Number of objects used for external prediction (test set).

<sup>h</sup> Models in which autoscaling pretreatment procedure was applied (+) and models in which raw data was used (–).

<sup>i</sup> Models in which inactive compounds (**S24–S33**, **S39**) were not included in training set nor in test set.

<sup>j</sup> Values in brackets were obtained using random groups cross validation procedure.

<sup>k</sup> Model was obtained using just ten compounds which were chosen as the representatives of the dataset according to the PCA results.

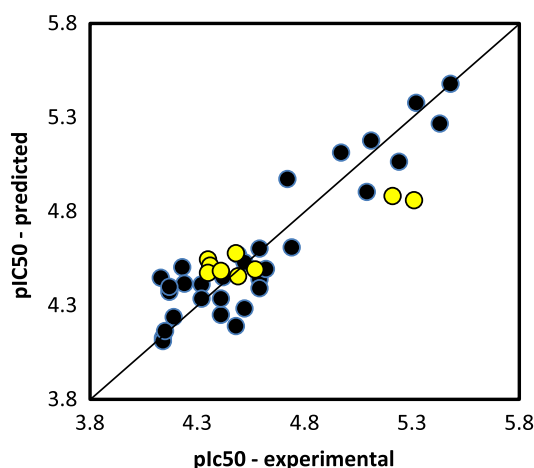


**Figure 1.** Predicted versus experimental antitumor activity, black dots present training set compounds, yellow dots present test set compounds.

actively correlated descriptors of the dataset compounds with the pIC<sub>50</sub> values higher than 5.00 (compounds **S41**, **S43**, **S45**, **S47–S51**) are: WN1–527.9 kcal/mol, W1–1587.5 kcal/mol, S–673.4 Å<sup>2</sup>, %FU10–2.6%. The average values of the same descriptors in the case of the least active dataset compounds used for building model **1** (**S1**, **S15**, **S17**, **S18**, **S21**, **S23**, **S35**), are: WN1–605.6 kcal/mol, W1–1432.1 kcal/mol, S–580.7 Å<sup>2</sup>, %FU10–78.1%.

## 2.2. Design of new compounds

Taking the advantage of previously reported structures,<sup>26–31</sup> all proposed compounds were designed with the same general core (1-arylmethyl-3-aryl-1H-pyrazole), fixed **A ring** and different modifications at position of **B ring** and **linker** (Fig. 4). Activity of each new, proposed compound was predicted using 3D-QSAR models and the most promising compounds were subjected to synthesis and biological tests (compounds **1–10**, Table 2).

Ring **A** contains 2-chloropyridine or *tert*-butylbenzyl in N-1 position since it was found that such compounds inhibited viability of A549 cell.<sup>27</sup> Modifications of **B ring** and **linker** were made in an attempt to emphasize properties that were found by 3D-QSAR analysis as positively correlated with antitumor activity. The most

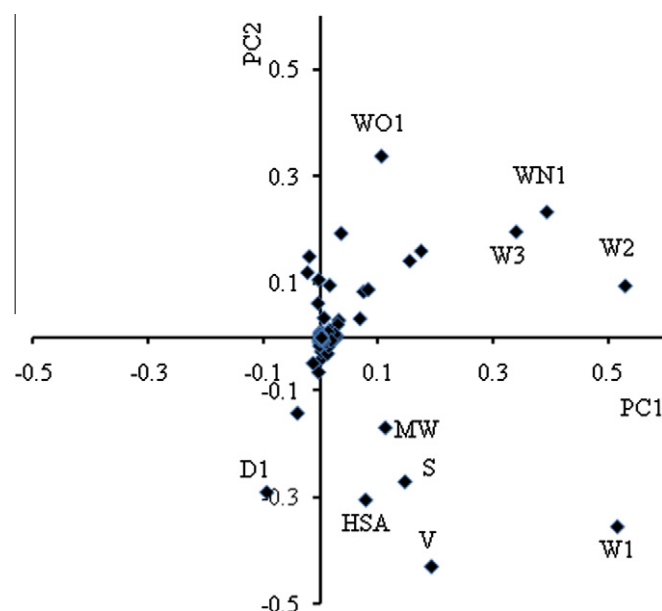


**Figure 2.** PCA loadings plot for the first two principal components. PCA was performed on the dataset used to build model **1**.

important descriptors with positive correlation to activity were related to polarizability and dispersion forces (W2, W3, W4). We assumed that introducing atoms with high electronegativity, such as oxygen, fluorine and nitrogen, into **B ring** of general formula (Fig. 4), would enhance these properties and improve biological activity. For that purpose compounds **1–6** were prepared. This modification also affected other descriptors with positive correlation to antitumor activity, such as molecular volume (V) and molecular mass (MW). Hydrophobic interactions (D1) were increased by introduction of additional aromatic ring. Further, the ability of a compound to make weak H-bond interaction with carbonyl group (WO1) and percentage of unionized species at pH 7 and 8 (%FU7, %FU8) were also found as descriptors with positive correlation to antitumor activity. Both factors indicate that presence of basic group is important. Thus, we replaced hydrazine group as basic linker with more basic amidooxime group. For that purpose compounds **7–10** were prepared. In addition, amidooxime

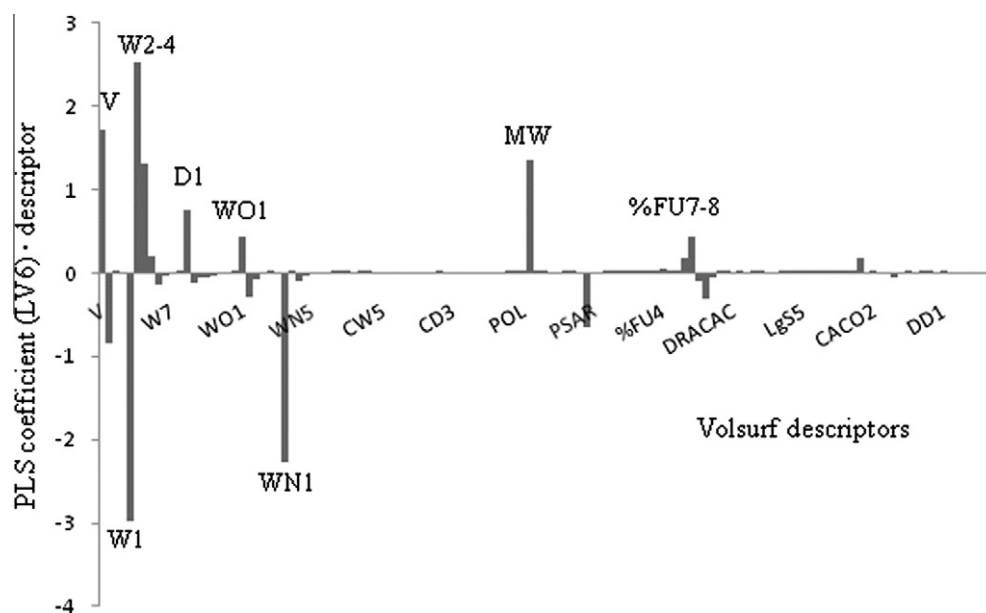


**Figure 3.** Products of the descriptor's average value (calculated for the dataset used to build the model) and the associated PLS coefficient of model 1. Descriptors with the highest impact on the activity are labeled; list and description of all 128 Volsurf+ descriptors is given in the VolSurf+ manual.<sup>32,33</sup>

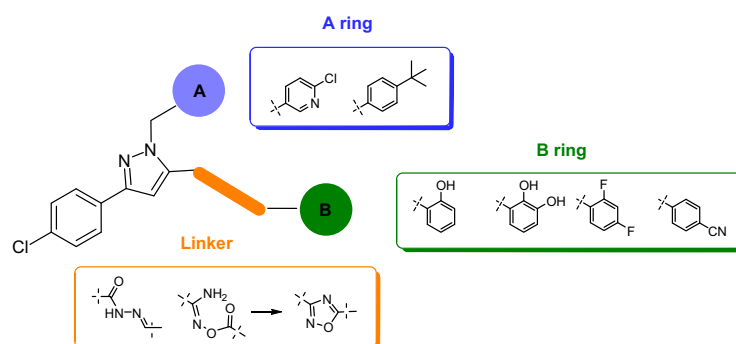


**Figure 4.** The common structural formula of the title compounds with colored portions indicated the modification sites.

compounds are able to complex with various metal ions<sup>35,36</sup> which is the property related with antitumor activity and chelation with ions in cell.<sup>27</sup> Finally, according to literature,<sup>37</sup> amidooxime group is less mutagenic and toxic than hydrazine group.

### 2.3. Chemistry

The synthetic pathways used for preparation of the tested compounds **1–10** (Table 2) are shown in Scheme 1 and Scheme 2. The starting material, ethyl 5-(4-chlorophenyl)-2*H*-pyrazole-3-carboxylate (**11**) was prepared from commercially available 4-substituted acetophenone and diethyl oxalate, with hydrazine in the presence of acetic acid at room temperature, according to procedures reported in literature.<sup>25,26</sup> In the next step, it was used for preparation of key intermediates **12a–b**, by alkylation with 2-chloro-5-chloromethylpyridine for **12a** and 1-*tert*-butyl-4-(chloromethyl)benzene for **12b**. We have applied rapid and efficient microwave irradiation for the synthesis of desired compounds **12a–b**. Compared to the conventional heating,<sup>26</sup> the reaction time was shortened to 30 min instead of 6–14 h. The reaction of intermediates **12a–b** with hydrazine hydrate gave carbonylhydrazide derivatives **13a–b** that were further treated with diverse aldehydes to afford final compounds **1–6** in good yields >80% (Scheme 1).

To prepare compounds **7–10** (Scheme 2), starting intermediates **12a–b**, were converted into corresponding acids **14a–b** by alkali

hydrolysis under microwave conditions at 110 °C for 30 min, then acylated with phosphorus chloride and finally converted to amides **15a–b** by introducing gaseous ammonia at room temperature. In the next step, amides **15a–b**, were converted into nitriles **16a–b** using POCl<sub>3</sub>. Reaction of the nitriles **16a–b** with hydroxylamine hydrochloride in the presence of triethylamine under microwave heating, afforded amidooxime derivatives **7** and **8** in a good yields. Finally, condensation of amidooxime **8** with 2,3-dihydroxybenzoic acid at room temperature afforded desired *O*-acylamidooxime **9**. However, at reflux temperature, with the same reagents, 1,2,4-oxadiazole derivative **10** was obtained as main product.

All newly synthesized compounds were characterized by spectral and LC–MS analyses which were in full agreement with the proposed structures.

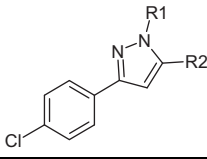
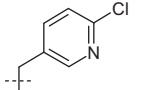
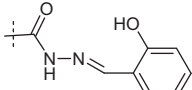
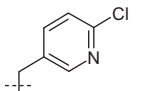
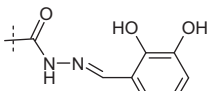
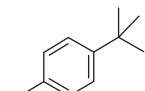
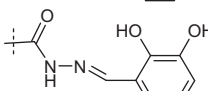
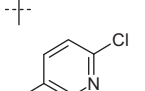
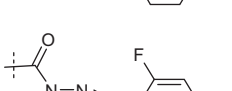
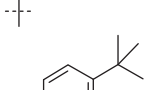
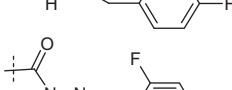
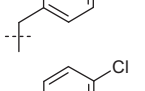
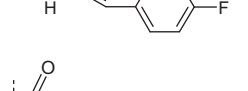
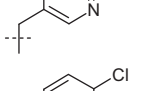
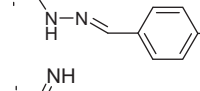
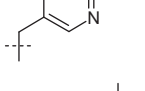
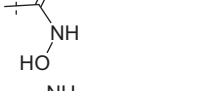
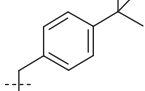
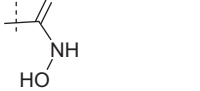
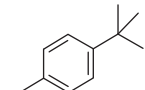
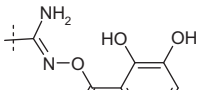
### 2.4. Biological evaluation

All prepared compounds **1–10** were tested on viability of A549 cell lines to compare predicted and experimental value (Table 2). In addition, all compounds were also tested on additional lung cancer cell line NCIH23 (adenocarcinoma, non-small cell lung cancer). These two cell lines, A549 and NCIH23, are adenocarcinomic human cell lines most commonly used in determination of antitumor screening activity of new chemical entities. While A549 cells are human cancer alveolar basal epithelial cells,



**Table 2**

New compounds, designed according to the results of 3D-QSAR analysis, and their predicted and measured antitumor activities against A549 lung cancer cells

Compound			Model 1 pIC <sub>50</sub> (μM) (pred) <sup>a</sup>	Model 2 pIC <sub>50</sub> (μM) (pred) <sup>a</sup>	MTS assay pIC <sub>50</sub> (μM) (exp) <sup>b</sup>
	R1	R2			
1			4.82	4.82	5.33
2			4.90	4.91	5.28
3			4.92	4.92	5.11
4			4.78	4.79	4.80
5			4.77	4.79	<4.00
6			4.77	4.81	<4.00
7			4.50	4.47	4.30
8			4.57	4.56	4.75
9			5.01	5.01	4.08
10			4.92	4.93	<4.00

<sup>a</sup> pIC<sub>50</sub> values of antitumor activity against A549 lung cancer cells predicted by model 1 and model 2.

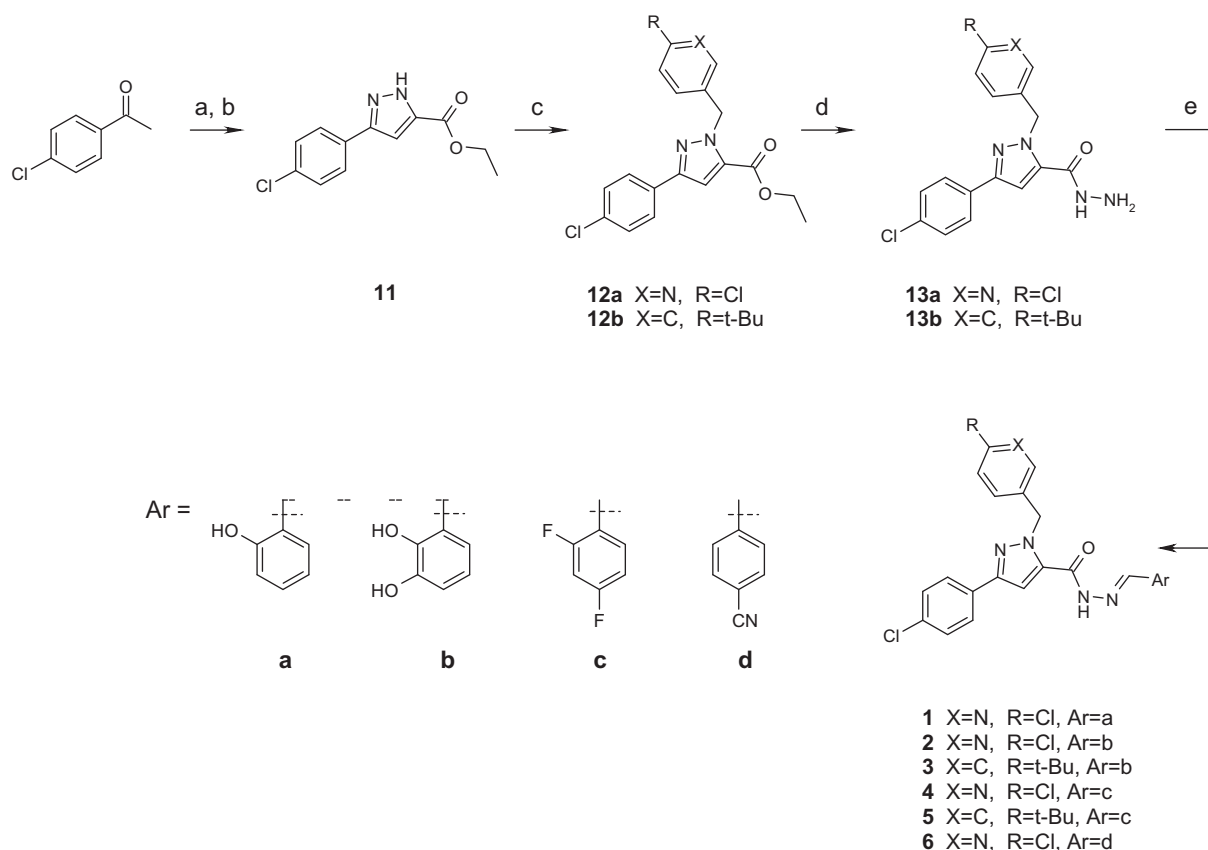
<sup>b</sup> pIC<sub>50</sub> values of antitumor activity against A549 lung cancer cells measured experimentally.

NCIH23 are lung cancer cells with K-ras and p53 gene mutations and high expression of c-myc gene, which are the most frequent events in process of carcinogenesis.<sup>38</sup>

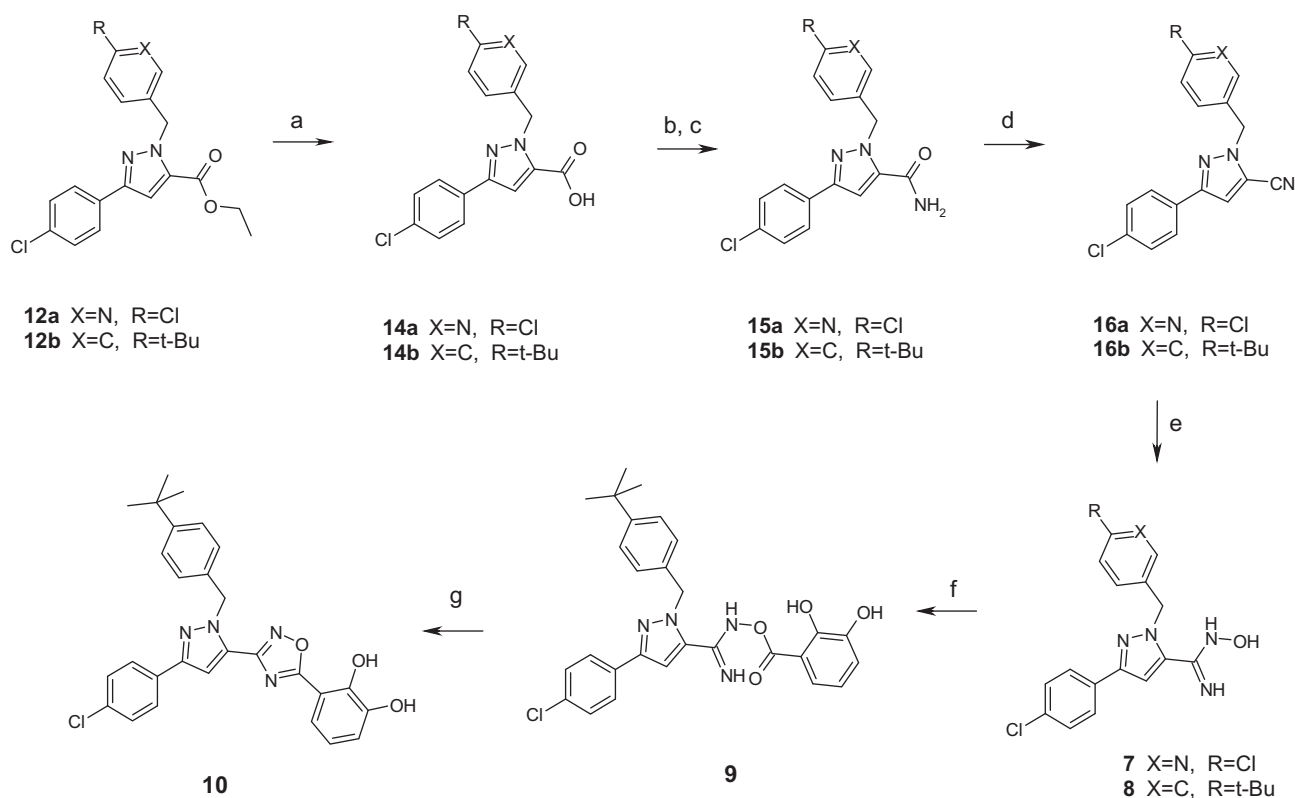
Influence of tested compounds on viability of A549 and NCIH23 cells was investigated using Promega MTS assay which measures metabolic activity of the cells and is widely used as a reliable way for measuring number of viable cells.<sup>39</sup> In this test, metabolic activity in cell population is measured via incubation with tetrasolium salt that is cleaved into a colored formazan product by metabolic active cells. Effect of new compounds on

proliferation of A549 and NCIH23 cancer cells was investigated by BrdU assay which measures incorporation of labeled DNA precursor 5-bromo-2'-deoxyuridine (BrdU) into genomic DNA during S phase of cell cycle. The results for each of tested compounds are reported as growth percentages compared with the untreated control cells after 48 h of drug exposure. IC<sub>50</sub> values were calculated using the program GraFit 5.0.12, and average values from three independent experiments are listed in Table 3.

Compound 1 was chosen as internal standard to test the compatibility of biological results found in literature<sup>27</sup> with our results.



**Scheme 1.** Reagents and conditions: (a) diethyl oxalate, NaOEt (21% in EtOH), rt, 10 min; (b) hydrazin hydrate, AcOH, rt, 30 min; (c) 2-chloro-5-(chloromethyl)pyridine or 1-(chloromethyl)-4-(1,1-dimethylethyl)benzene, K<sub>2</sub>CO<sub>3</sub>, CH<sub>3</sub>CN, microwave, 120 °C, 30 min; (d) hydrazine hydrate, MeOH, 65 °C, 24 h; (e) aldehyde, EtOH, 30 °C, 5 h.



**Scheme 2.** Reagents and conditions: (a) NaOH, EtOH, microwave, 110 °C, 30 min; (b) POCl<sub>3</sub>, 120 °C, 2 h; (c) NH<sub>3</sub> gas, THF, rt, 20 min; (d) POCl<sub>3</sub>, pyridine, rt, 2 h; (e) hydroxyamine hydrochloride, Et<sub>3</sub>N, EtOH, microwave, 80 °C, 30 min; (f) DCC, DMAP, CH<sub>3</sub>CN, carboxylic acid, rt, 24 h; (g) DCC, DMAP, CH<sub>3</sub>CN, carboxylic acid, 50 °C, 24 h.



Excellent correlation between published data and our measurement of its activity was obtained (Table 3). Due to later, compound **1** was found to be a good system for evaluation of newly synthesized compounds.

Results obtained by MTS and BrdU assays (Table 3) showed similar effects of the new compounds on growth of both, A549 and NCIH23, cell lines. Exception is compound **5** which is inactive on viability and proliferating assay on A549, inactive in viability assay on NCIH23, but active on proliferative BrdU assay and therefore need further profiling. Also, compound **6** was not active in both assays (due to low solubility). For all compounds, inhibition of growth measured with MTS assay has higher  $IC_{50}$  values than inhibition measured with BrdU assay. Compounds **1**, **2**, **3**, **4**, **7** and **9** are active on both cell lines and inhibit growth as well as proliferation of cell population. Compound **8** showed the same range of growth inhibition in metabolic and proliferating assays. Compound **10** showed no activity in MTS assay on both cell lines, but showed strong activity in proliferation BrdU assay for both cell lines. This results points to the absence of cytotoxic activity and potential cytostatic activity of compound **10**.

### 2.5. Anticancer activity of new pyrazole derivative

Comparison of predicted and experimentally measured antitumor activities of new compounds using MTS assay is presented in Table 2. Very good agreement between measured and predicted activities was observed for compound **1**. Introduction of additional hydroxyl group into compound **1**, led to compounds **2** and **3** which were experimentally determined as the most potent ones, even more active than it was predicted ( $pIC_{50}$ -pred = 4.90,  $pIC_{50}$ -exp = 5.28 and  $pIC_{50}$ -pred = 4.92,  $pIC_{50}$ -exp = 5.11, respectively). Also, compounds **2** and **3**, are colored yellow and that can potentially interfere with readouts of MTS assay. The same problem is not connected to the BrdU proliferative assay (Table 3). Complete agreement between predicted and experimentally determined activity was obtained for compound **4** ( $pIC_{50}$ -pred = 4.78,  $pIC_{50}$ -exp = 4.80), which was obtained from compound **2** by substitution of hydroxyl groups with fluorine atoms. Its activity demonstrates that it is possible to substitute hydroxyl group liable to glucoronization with more drug-like fluoro group<sup>40</sup> and to maintain activity. Unfortunately, *tert*-butylbenzyl analogue **5**, proved to be inactive on viability and proliferating assay on A549 (Table 3). Its inactivity is probably consequence of its strong tendency to precipitate in culture media, which implies that compound **5** might be active due to structural features, but because of insolubility in aqueous media it is impossible to experimentally determine its activity. Since compound **5** showed some activity on inhibition of proliferation of NCIH23 (Table 3), its further profiling is needed. The compound **6** was not active in both assays (Table 3). Its inactivity could be attributed to very low solubility in DMSO media. Fair correlation

between predicted and measured activity was obtained for compounds **7** and **8** (Table 2). Their activities are particularly interesting because these derivatives do not contain **B** ring, a structural feature present in all other structures, and hydrazine linker was replaced with amidooxime linker. Therefore, the good inhibitory activity of **7** and **8** is mostly determined by compound basicity and possibility to make weak H-bond interactions with carbonyl group, properties provided by amidooxime substitution. Acylation of compound **8** led to compound **9** which have been predicted as strongly active compound. Surprisingly, it showed lower activity on viability test against A549 cells than reference compound **1** and parent compound **8**. Possible explanation for lower activity of **9** in MTS assay than it was predicted could be its spontaneous conversion into compound **10**. During preparation of compound **9**, it was noticed that higher temperature or prolonged time of stirring (>24 h) afforded compound **10** as main product. Since compound **10** shows no activity on inhibition of A549 cell lines (Table 3), it is very likely that lower activity of **9** is consequence of its partial conversion into **10**. However, compound **9** demonstrated high proliferation inhibition on A549 cell line and showed notable activity on both cells assays in case of NCIH23 cell line. These results showed importance of different in vitro assays for more accurate evaluation of biological activity.

Finally, compound **10**, as the only one with rigid linker in the structure, proved to be the most interesting compound from therapeutic point of view. Compound **10** showed low activities in MTS assays, but it showed high activities in BrdU assays (Table 3). Significant activities in BrdU assays reveal its potential cytostatic activity that, in combination with absence or very low cytotoxic activity, makes this compound a good starting point for further design of new, more potent and safer anticancer therapeutics.

### 3. Conclusion

The presented studies demonstrate how 3D-QSAR analysis can serve as a guideline for synthesis of new compounds. Apparently, such approach proved to be useful in planning experiments and it made experimental search for new compounds with antitumor activity more efficient and faster. Predicted activities were in accordance with experimentally determined ones for the majority of compounds. In some cases, discrepancy between predicted and measured activities was caused by low solubility of the compounds in the media used for biological tests.

Antitumor activities of new pyrazole derivatives showed that hydroxy and hydrazine groups (which might be responsible for metabolic instability and toxic effect) can be substituted with fluorine and amidooxime, respectively, without affecting the activity. Substitution of hydrazine linker with rigid, 1,2,4-oxadiazoline moiety resulted with the most interesting compound from the therapeutic point of view according to the additional biological evaluation. Although compound **10** was inactive on inhibition of A549 cells, it was found to have potential cytostatic activity due to observed significant activities in BrdU assays. The later, together with its low (if any) cytotoxic activity, makes compound **10** a promising lead compound for future design of new anticancer therapeutics.

### 4. Experimental section

#### 4.1. D-QSAR analysis

##### 4.1.1. Dataset

Dataset of 51 compounds<sup>25–28</sup> with measured antitumor activity against A549 lung cancer cells, (Table S1 in Supplementary data), was used for building and validation of 3D-QSAR models.

**Table 3**  
Growth inhibitory and cell proliferation ( $IC_{50}$ ) of A549 and NCIH23 cells for the compounds **1–10** at 48 h

Compound	A549		NCIH23	
	MTS assay $IC_{50}$ ( $\mu$ M)	BrdU assay $IC_{50}$ ( $\mu$ M)	MTS assay $IC_{50}$ ( $\mu$ M)	BrdU assay $IC_{50}$ ( $\mu$ M)
<b>1</b>	4.70	0.30	3.04	0.27
<b>2</b>	5.20	0.70	3.35	0.57
<b>3</b>	7.80	0.40	3.91	0.3
<b>4</b>	16.01	9.05	13.50	7.86
<b>5</b>	>100	>100	>100	21.88
<b>6</b>	>100	>100	>100	>100
<b>7</b>	50.50	38.29	44.39	27.94
<b>8</b>	17.70	17.00	16.49	12.28
<b>9</b>	83.22	26.75	21.88	15.63
<b>10</b>	>100	1.54	>100	0.36

All the compounds from the dataset have common structural features, 1-arylmethyl-3-aryl-1*H*-pyrazole as the main core, while modifications were made at position N1, C3 and C5 where differently substituted aromatic rings were introduced. Negative logarithmic value ( $\text{pIC}_{50}$ ) of measured antitumor activities was used in deriving 3D-QSAR models. For the inactive compounds whose  $\text{IC}_{50}$  values are not explicitly given in the literature, but just stated as inactive or estimated as  $>5 \times 10^{-4} \text{ mol/dm}^3$ ,  $\text{pIC}_{50}$  was set to 3.30.

#### 4.1.2. Calculation of molecular descriptors

For each compound, 3D structure was generated using VolSurf+ program<sup>32,33</sup> and Molecular Interaction Fields (MIFs) were calculated by the program GRID.<sup>41</sup> Grid spacing was set to 0.5 Å and the following probes were used: H<sub>2</sub>O (the water molecule), O ( $\text{sp}^2$  carbonyl oxygen atom), N1 (neutral NH group (e.g., amide)) and DRY (the hydrophobic probe). From the MIFs, VolSurf+ derived series of 128 descriptors (independent of molecular alignment) that refer to molecular size and shape, to hydrophilic and hydrophobic regions and to the balance between them, to the 'charge state', to lipophilicity, and molecular diffusion,  $\log P$ ,  $\log D$ , to the presence/distribution of pharmacophoric groups as well as to some other relevant ADME properties. VolSurf+ descriptors are based on 3-D Molecular Interaction Fields, but are compressed to alignment independent descriptors. The definition of all 128 VolSurf+ descriptors is given in the VolSurf+ manual.<sup>32,33</sup>

#### 4.1.3. Building and validation of 3D-QSAR models

The relationship between the structure based molecular descriptors and biological activity of the dataset compounds was determined using the partial least square (PLS) analysis. The number of significant latent variables (nLV) and quality of the models were determined using the leave-one-out (LOO) and random group's cross-validation procedures. In the later case, 5 random groups and 30 iterations were used. Standard deviation of error of calculation (SDEC) and standard deviation of error of prediction (SDEP) were calculated for each model. In order to make more realistic validation of the predictive power of the models, external validation was also performed. For that purpose, dataset compounds were divided into training set (used to build the model) and test set (used for external prediction). Test set compounds were randomly chosen from the overall dataset using random number generator ([www.random.org](http://www.random.org)). The size of the test set was approximately 1/4 of the overall dataset. The SDEP for external validation was calculated using homemade program. In order to identify the descriptors with the highest (positive or negative) impact on biological activity of the compounds, products between PLS coefficient and average value of the descriptor were observed. Similar approach for identifying the most important descriptors has been used in investigation of *P*-glycoprotein interacting drugs.<sup>42</sup>

In deriving QSAR models, both pretreatment procedures that are available in VolSurf+ program (raw and autoscaling) were tested. Using the autoscaling pretreatment every variable is mean centered and scaled to give it unit variance. With raw pretreatment procedure, raw data matrix is used. Also, models that include inactive compounds, as well as the models without inactive compounds were derived (Table 1).

Principal component analysis (PCA) was performed on the molecular descriptors of dataset compounds used for building models 1 and 2. PCA loadings were used for identifying the descriptors with the highest contribution to the first two principal components. Usefulness of PCA in QSAR analysis has already been proved in several cases.<sup>31,43</sup>

## 4.2. Chemistry

All solvents and reagents were used as supplied, unless noted otherwise. Yields given are isolated yields. NMR spectra were recorded at 25 °C in DMSO-*d*<sub>6</sub> with TMS as the internal standard on Bruker Avance DRX500 spectrometer equipped with 5 mm diameter inverse detection probe with z-gradient accessory, as well as Bruker Avance DPX300 spectrometer using dual <sup>1</sup>H probe. Melting points were obtained using a Kofler apparatus and are uncorrected. Mass spectra were recorded on Varian MAT 311 instrument (FAB), and Platform LCZ or LCQ Deca instruments (ESI). The analyses were performed using the following condition: An Acquity UPLC BEH C18 analytical column (50 mm × 2.1 mm, 1.7 μm packing diameter) on Quattro micro™ (Micromass) mass spectrometer, using external calibration) with the following two solvents; solvent A, 0.1% v/v solution of formic acid in water; solvent B, 0.1% v/v solution of formic acid in acetonitrile; start 97% A, linear gradient to 100% B in 1.5 min, then 0.4 min at 100% B, then linear gradient to 97% A in 0.1 min. Total run time 2 min. All tested compounds have a purity of at least 90% according to NMR and UPLC analyses.

### 4.2.1. General procedure for the synthesis of 1–6

The mixture of carbohydrazide **13a-b** (0.1 mmol) and corresponding aldehyde (0.1 mmol) in EtOH (1 ml) was stirred at 30 °C for 5 h. The reaction mixture was concentrated under reduced pressure and purified by flash chromatography (0–100% EtOAc/cyclohexane) affording **1–6** as pure compounds.

#### 4.2.1.1. 3-(4-Chlorophenyl)-1-[(6-chloro-3-pyridinyl)methyl]-*N*-[(1*E*)-(2-hydroxyphenyl)methylidene]-1*H*-pyrazole-5-carbohydrazide (1).

The title compound **1** was obtained as a white solid, from carbohydrazide **13a** and 2-hydroxybenzaldehyde following the general procedure described above. Yield: 92%; mp 231–233 °C;<sup>27</sup> <sup>1</sup>H NMR (500 MHz, DMSO)  $\delta$ : 5.82 (s, 2H, CH<sub>2</sub>), 6.85–6.99 (m, 2H, 5-ArH), 7.32 (t, 1H, 5-ArH), 7.46–7.57 (m, 4H, 1-ArH, 3-ArH), 7.59–7.61 (m, 1H, 5-ArH), 7.75 (d, 1H, *J* = 7.35, 1-ArH), 7.82 (d, 2H, *J* = 8.35, 3-ArH), 8.39 (s, 1H, 1-ArH), 8.64 (s, 1H, =CH), 10.93 (s, 1H, OH), 12.20 (s, 1H, NH); <sup>13</sup>C NMR (125 MHz, DMSO)  $\delta$ : 51.2, 105.5, 116.5, 118.8, 119.5, 124.4, 126.9, 128.9, 129.0, 130.9, 131.8, 132.7, 132.8, 135.4, 139.1, 148.3, 148.5, 149.1, 149.5, 155.2, 157.4; MS (ESI): *m/z* (94%) 466.0 [M+H]<sup>+</sup>.

#### 4.2.1.2. 3-(4-Chlorophenyl)-1-[(6-chloro-3-pyridinyl)methyl]-*N*-[(1*E*)-(2,3-dihydroxy-phenyl)methylidene]-1*H*-pyrazole-5-carbohydrazide (2).

The title compound **2** was obtained as a yellow solid, from carbohydrazide **13a** and 2,3-dihydroxybenzaldehyde following the general procedure described above. Yield: 95%; mp 150–152 °C; <sup>1</sup>H NMR (500 MHz, DMSO)  $\delta$ : 5.85 (s, 2H, CH<sub>2</sub>), 6.73 (t, 1H, 5-ArH), 6.86 (d, 1H, *J* = 7.60, 5-ArH), 7.02 (d, 1H, *J* = 7.60, 5-ArH), 7.48–7.54 (m, 4H, 3-ArH, 1-ArH, 4-H), 7.73–7.78 (m, 1H, 1-ArH), 7.82 (d, 2H, *J* = 8.36, 3-ArH), 8.38 (s, 1H, 1-ArH), 8.61 (s, 1H, =CH), 9.35 (s, 1H, OH), 10.62 (s, 1H, OH), 12.17 (s, 1H, NH); <sup>13</sup>C NMR (125 MHz, DMSO)  $\delta$ : 51.2, 105.5, 117.5, 119.0, 119.3, 124.4, 126.9, 128.9, 129.0, 130.9, 132.7, 132.8, 135.4, 139.1, 145.7, 146.1, 148.3, 148.5, 149.1, 149.5, 155.2; MS (ESI): *m/z* (100%) 482.0 [M+H]<sup>+</sup>.

#### 4.2.1.3. 3-(4-Chlorophenyl)-*N*-[(1*E*)-(2,3-dihydroxyphenyl)methylidene]-1-[[4-(1,1-dimethylethyl)phenyl]methyl]-1*H*-pyrazole-5-carbohydrazide (3).

The title compound **3** was obtained as a yellow solid, from carbohydrazide **13b** and 2,3-dihydroxybenzaldehyde following the general procedure described above. Yield: 92%; <sup>1</sup>H NMR (500 MHz, DMSO)  $\delta$ : 1.23 (s, 9H, 3Me), 5.77 (s, 2H, CH<sub>2</sub>), 6.73 (t, 1H, 5-ArH), 6.83–6.88 (m, 1H, 5-ArH), 6.98–7.04 (m, 1H, 5-ArH), 7.20 (d, 2H, *J* = 7.90, 1-ArH), 7.34 (d, 2H, *J* = 7.90, 1-ArH), 7.49 (t, 1H, 4-H), 7.52 (d, 2H, *J* = 8.35, 3-

ArH), 7.82 (d, 2H,  $J$  = 8.35, 3-ArH), 8.60 (s, 1H, =CH), 9.31 (s, 1H, OH), 10.56 (s, 1H, OH), 12.15 (s, 1H, NH);  $^{13}\text{C}$  NMR (125 MHz, DMSO)  $\delta$ : 31.1, 34.3, 53.7, 105.5, 117.5, 119.0, 119.3, 125.2, 126.9, 127.2, 128.9, 129.0, 130.9, 132.7, 134.1, 135.4, 145.7, 146.1, 148.3, 148.5, 150.3, 155.2; MS (ESI):  $m/z$  (98%) 501.3 [M+H] $^{+}$ .

**4.2.1.4. 3-(4-Chlorophenyl)-1-[(6-chloro-3-pyridinyl)methyl]-*N*-[(1*E*)-(2,4-difluorophenyl)methylidene]-1*H*-pyrazole-5-carbohydrazide (4).**

The title compound **4** was obtained as a white solid, from carbohydrazide **13a** and 2,4-difluorobenzaldehyde following the general procedure described above. Yield: 80%; mp 218–221 °C;  $^1\text{H}$  NMR (300 MHz, DMSO)  $\delta$ : 5.81 (s, 2H, CH<sub>2</sub>), 7.22 (t, 1H, 5-ArH), 7.39 (t, 1H, 5-ArH), 7.45–7.57 (m, 4H, 3-ArH, 1-ArH, 4-H), 7.69–7.77 (m, 1H, 1-ArH), 7.82 (d, 2H,  $J$  = 8.28, 3-ArH), 7.90–8.04 (m, 1H, 5-ArH), 8.37 (s, 1H, 1-ArH), 8.59 (s, 1H, =CH), 12.25 (s, 1H, NH);  $^{13}\text{C}$  NMR (75 MHz, DMSO)  $\delta$ : 51.2, 104.6, 105.5, 112.7, 112.9, 118.4, 124.4, 126.9, 128.0, 129.0, 130.9, 132.6, 132.8, 135.5, 139.1, 140.7, 148.5, 149.1, 149.6, 155.5, 162.6; MS (ESI):  $m/z$  (97%) 486.0 [M+H] $^{+}$ .

**4.2.1.5. 3-(4-Chlorophenyl)-*N*'-[(1*E*)-(2,4-difluorophenyl)methylidene]-1-[[4-(1,1-dimethylethyl)phenyl]methyl]-1*H*-pyrazole-5-carbohydrazide (5).**

The title compound **5** was obtained as a white solid, from carbohydrazide **13b** and 2,4-difluorobenzaldehyde following the general procedure described above. Yield: 78%; mp 74–76 °C;  $^1\text{H}$  NMR (300 MHz, DMSO)  $\delta$ : 1.21 (s, 9H, 3Me), 5.74 (s, 2H, CH<sub>2</sub>), 7.11–7.25 (m, 3H, 1-ArH, 5-ArH), 7.26–7.42 (m, 3H, 1-ArH, 5-ArH), 7.43–7.57 (m, 3H, 3-ArH, 4-H), 7.81 (d, 2H,  $J$  = 8.35, 3-ArH), 7.90–8.03 (m, 1H, 5-ArH), 8.58 (s, 1H, =CH), 12.06 (s, 1H, NH);  $^{13}\text{C}$  NMR (75 MHz, DMSO)  $\delta$ : 31.2, 34.3, 54.2, 104.6, 105.5, 112.7, 112.9, 118.4, 125.4, 126.9, 127.1, 128.0, 129.0, 130.9, 132.6, 134.0, 135.5, 140.7, 148.5, 150.2, 155.5, 162.6; MS (ESI):  $m/z$  (100%) 507.5 [M+H] $^{+}$ .

**4.2.1.6. 3-(4-Chlorophenyl)-1-[(6-chloro-3-pyridinyl)methyl]-*N*'-[(1*E*)-(4-cyanophenyl)methylidene]-1*H*-pyrazole-5-carbohydrazide (6).**

The title compound **6** was obtained as a white solid, from carbohydrazide **13a** and 4-formylbenzonitrile following the general procedure described above. Yield: 84%; mp 238–240 °C;  $^1\text{H}$  NMR (300 MHz, DMSO)  $\delta$ : 5.80 (s, 2H, CH<sub>2</sub>), 7.44–7.56 (m, 4H, 5-ArH), 7.70–7.77 (m, 1H, 4-H), 7.78–7.82 (m, 2H, 1-ArH), 7.92 (s, 4H, 3-ArH), 8.36 (s, 1H, 1-ArH), 8.45 (s, 1H, =CH), 12.24 (s, 1H, NH);  $^{13}\text{C}$  NMR (75 MHz, DMSO)  $\delta$ : 51.2, 59.8, 105.5, 112.2, 118.6, 124.4, 126.9, 127.8, 129.0, 130.9, 132.7, 132.8, 135.4, 138.2, 138.4, 139.1, 146.7, 148.5, 149.1, 149.5; MS (ESI):  $m/z$  (97%) 475.0 [M+H] $^{+}$ .

**4.2.2. Synthesis of compounds 7–10**

**4.2.2.1. 3-(4-Chlorophenyl)-1-[(6-chloro-3-pyridinyl)methyl]-*N*-hydroxy-1*H*-pyrazole-5-carboximidamide (7).**

A mixture of **16a** (54 mg, 0.16 mmol), hydroxyamine hydrochloride (34 mg, 0.49 mmol) and Et<sub>3</sub>N (0.22 ml, 1.6 mmol) in ethanol (4 ml) was heated under microwave irradiation at 80 °C for 30 min. After reaction was concentrated the residue was purified by flash chromatography (0–100% EtOAc/cyclohexane) to afford pure **7** (47 mg, 80%) as a white solid; mp 170–172 °C;  $^1\text{H}$  NMR (300 MHz, DMSO)  $\delta$ : 5.69 (s, 2H, CH<sub>2</sub>), 6.01 (s, 2H, NH, OH), 7.16 (s, 1H, 4-H), 7.42–7.52 (m, 3H, 1-ArH, 3-ArH), 7.65–7.67 (m, 1H, 1-ArH), 7.76 (d, 2H,  $J$  = 8.50, 3-ArH), 8.30–8.34 (m, 1H, 1-ArH), 9.95 (s, 1H, NH);  $^{13}\text{C}$  NMR (75 MHz, DMSO)  $\delta$ : 51.0, 103.9, 124.2, 126.7, 128.8, 131.5, 132.3, 132.9, 137.5, 138.9, 144.3, 148.6, 149.0, 149.3; MS (ESI):  $m/z$  (100%) 362.3 [M+H] $^{+}$ .

**4.2.2.2. 3-(4-Chlorophenyl)-1-[[4-(1,1-dimethylethyl)phenyl]methyl]-*N*-hydroxy-1*H*-pyrazole-5-carboximidamide (8).**

The title compound **8** (41 mg, 74%) was obtained as a

white solid, from **16b** (50 mg, 0.14 mmol), following the method described for **7**.

$^1\text{H}$  NMR (300 MHz, DMSO)  $\delta$ : 1.23 (s, 9H, 3Me), 5.63 (s, 2H, CH<sub>2</sub>), 5.95 (s, 2H, NH, OH), 7.06–7.15 (m, 3H, 4-H, 1-ArH), 7.26–7.33 (m, 2H, 1-ArH), 7.45 (d, 2H,  $J$  = 8.52, 3-ArH), 7.76 (d, 2H,  $J$  = 8.52, 3-ArH), 9.88 (s, 1H, NH);  $^{13}\text{C}$  NMR (75 MHz, DMSO)  $\delta$ : 31.1, 34.2, 54.3, 104.1, 125.4, 126.8, 127.1, 128.9, 131.4, 132.3, 134.1, 137.3, 144.2, 148.5, 150.1; MS (ESI):  $m/z$  (90%) 383.4 [M+H] $^{+}$ .

**4.2.2.3. 3-[3-(3-(4-Chlorophenyl)-1-[[4-(1,1-dimethylethyl)phenyl]methyl]-1*H*-pyrazol-5-yl)-1,2,4-oxadiazol-5-yl]-1,2-benzenediol (9).**

To a solution of amidooxime **8** (15.3 mg, 0.04 mmol), *N,N*-dicyclohexylcarbodiimide DCC (8.5 mg, 0.041 mmol) and dimethylaminopyridine DMAP (0.4 mg, 0.0032 mmol) in dry acetonitrile (1.5 ml) was added carboxylic acid (6.3 mg, 0.041 mmol) under vigorous stirring. The reaction mixture was stirred at rt for 24 h. After reaction was concentrated the residue was purified by flash chromatography (0–100% EtOAc/cyclohexane) to afford pure **9** (12 mg, 58%) as a white solid.

$^1\text{H}$  NMR (300 MHz, DMSO)  $\delta$ : 1.22 (s, 9H, 3Me), 5.55 (d, 2H, 2xNH), 5.85 (s, 2H, CH<sub>2</sub>), 6.77 (t, 1H, 5-ArH), 7.04 (d, 1H,  $J$  = 7.50, 5-ArH), 7.20 (s, 1H, 4-H), 7.25–7.38 (m, 4H, 1-ArH), 7.48 (d, 2H,  $J$  = 8.50, 3-ArH), 7.62 (d, 1H,  $J$  = 7.50, 5-ArH), 7.81 (d, 2H,  $J$  = 8.50, 3-ArH), 9.48 (s, 1H, OH), 10.46 (s, 1H, OH);  $^{13}\text{C}$  NMR (75 MHz, DMSO)  $\delta$ : 31.1, 34.2, 54.3, 104.1, 117.4, 119.1, 119.3, 125.4, 126.8, 127.1, 128.9, 131.4, 132.3, 134.1, 137.3, 145.7, 146.1, 146.4, 148.5, 150.1, 155.6, 174.2; MS (ESI):  $m/z$  (93%) 519.4 [M+H] $^{+}$ .

**4.2.2.4. 3-[3-(3-(4-Chlorophenyl)-1-[[4-(1,1-dimethylethyl)phenyl]methyl]-1*H*-pyrazol-5-yl)-1,2,4-oxadiazol-5-yl]-1,2-benzenediol (10).**

To a solution of amidooxime **8** (15.3 mg, 0.04 mmol), *N,N*-dicyclohexylcarbodiimide DCC (8.5 mg, 0.041 mmol) and dimethylaminopyridine DMAP (0.4 mg, 0.0032 mmol) in dry acetonitrile (1.5 ml) was added carboxylic acid (6.3 mg, 0.041 mmol) under vigorous stirring. The reaction mixture was stirred at 120 °C for 4 h. After reaction was concentrated the residue was purified by flash chromatography (0–100% EtOAc/cyclohexane) to afford pure **10** (15 mg, 74%) as a white solid.

$^1\text{H}$  NMR (500 MHz, DMSO)  $\delta$ : 1.22 (s, 9H, 3Me), 5.85 (s, 2H, CH<sub>2</sub>), 7.14 (d, 1H,  $J$  = 8.30, 5-ArH), 7.22 (d, 2H,  $J$  = 8.30, 1-ArH), 7.33 (d, 2H,  $J$  = 8.30, 1-ArH), 7.50 (d, 2H,  $J$  = 8.50, 3-ArH), 7.55 (t, 1H, 5-ArH), 7.62 (1, 1H, 4-H), 7.96 (d, 2H,  $J$  = 8.50, 3-ArH), 8.01 (d, 1H,  $J$  = 7.50, 5-ArH), 9.40 (s, 1H, OH), 10.74 (s, 1H, OH);  $^{13}\text{C}$  NMR (125 MHz, DMSO)  $\delta$ : 31.1, 34.2, 54.3, 106.7, 117.5, 119.0, 119.3, 125.4, 127.0, 127.1, 128.8, 130.4, 132.7, 134.0, 135.1, 145.7, 146.1, 149.5, 150.1, 157.4, 160.1, 175.0; MS (ESI):  $m/z$  (98%) 501.3 [M+H] $^{+}$ .

**4.3. Biology**

**4.3.1. Cell culture**

The human cancer cell lines A549 and NCIH23 were purchased from ATCC and grown in ATCC recommended cell media supplemented with 10% heat-inactivated fetal calf serum (BIOWEST<sup>®</sup> Cat. No.: S181) and 1% antibiotic-antimycotic (Gibco, Cat. No. 15240-062) in an atmosphere of 5% CO<sub>2</sub> at 37 °C. A549 cells were grown in F12K Nutrient Mixture Kaighn's modification (Cat. No. 21127022), and NCIH23 in RPMI Medium 1640 (GIBCO Cat. No. A10491-01). All proliferation assays were performed in RPMI 1640 medium.

**4.3.2. Compound preparation**

All tested compounds were dissolved in DMSO to obtain 10 mM stock solutions. Final concentrations of tested compounds were in range of 100–0.2  $\mu\text{M}$  and with constant concentration of 1% DMSO at all compound dilutions.

### 4.3.3. MTS assay

Cancer cells were seeded at concentration of  $5 \times 10^3$  in 96 well-flat bottom plates in medium F12 K (A549) or RPMI1640 (NCIH23) culture medium supplemented with 10% FBS and incubated in an atmosphere of 5% CO<sub>2</sub> at 37 °C for 3 h. The cells were then treated with tested compounds at final concentrations of 100–0.2 μM for 48 h. After incubation cell proliferation and viability was measured by the (3-(4,5-dimethylthiazol-2-yl)-5-(3-carboxymethoxyphenyl)-2-(4-sulfophenyl)*H*-tetrazolium, inner salt; MTS based assay (Promega). Twenty microliters of MTS solution was added to the cells and incubated at 37 °C in CO<sub>2</sub> incubator. The conversion of MTS into aqueous soluble formazan is accomplished by dehydrogenase enzymes found in metabolically active cells. The quantity of formazan product measured by the amount of 490 nm absorbance is directly proportional to the number of living cells in culture.

### 4.3.4. BrdU assay (Amersham cell proliferation Biotrak ELISA system, RPN250)

Cancer cells were seeded at concentration of  $5 \times 10^3$  in 96 well-flat bottom plates in medium RPMI1640 (GIBCO Cat. No. A10491-01) supplemented with 10% FBS and incubated in an atmosphere of 5% CO<sub>2</sub> at 37 °C for 3 h. The cells were then treated with tested compounds at final concentrations of 100–0.2 μM for 48 h. BrdU was added to the cells in final concentration of 10 μM and reincubated for 3 h. During the labeling period the pyrimidine analogue BrdU is incorporated in place of thymidine into DNA of proliferating cells. After removing the culture medium the cells are fixed and the DNA denatured for 30 min at rt. Solution for fixation was removed and cells were treated with 200 μl of blocking reagents for 30 min at rt following treatment with 100 μl peroxidase labeled BrdU solution for 90 min. The immune complexes are detected by the subsequent substrate reaction and the resultant color was read at 450 nm using Envision plate reader. The absorbance values correlate directly to the amount of DNA synthesis and thereby to the number of proliferating cells. Reduction of DNA synthesis was calculated relative to control (untreated cells), the IC<sub>50</sub> values were calculated using GraFit 5.0.12 software.

### Acknowledgment

We gratefully acknowledge support by the Ministry of Science, Education and Sport of the Republic of Croatia (Projects 098-1191344-2860 and 098-0982933-2911).

### Supplementary data

Supplementary data associated with this article can be found, in the online version, at doi:10.1016/j.bmc.2012.01.032.

### References and notes

1. An Ipsos MORI report for the Global Lung Cancer Coalition, June 2010.
2. Jemal, A.; Siegel, R.; Xu, J.; Ward, E. *CA Cancer J. Clin.* **2010**, *60*, 277.
3. Seymour, L. *Cancer Treat. Rev.* **1999**, *25*, 301.
4. Tietze, L. F.; Steinmetz, A.; Balkenhohl, F. *Bioorg. Med. Chem. Lett.* **1997**, *7*, 1303.
5. Grosche, P.; Holtzel, A.; Walk, T. B.; Trautwein, A. W.; Jung, G. *Synthesis* **1961**, 1999.
6. Penning, T. D.; Talley, J. J.; Bertenshaw, S. R.; Carter, J. S.; Collins, P. W.; Docter, S.; Graneto, M. J.; Lee, L. F.; Malecha, J. W.; Miyashiro, J. M.; Rogers, R. S.; Rogier, D. J.; Yu, S. S.; Anderson, G. D.; Burton, E. G.; Cogburn, J. N.; Gregory, S. A.; Koboldt, C. M.; Perkins, W. E.; Seibert, K.; Veenhuizen, A. W.; Zhang, Y. Y.; Isakson, P. C. *J. Med. Chem.* **1997**, *40*, 1347.

7. Regan, J.; Breitfelder, S.; Cirillo, P.; Gilmore, T.; Graham, A. G.; Hickey, E.; Klaus, B.; Madwed, J.; Moriak, M.; Moss, N.; Pargellis, C.; Pav, S.; Proto, A.; Swinamer, A.; Tang, L.; Torcellini, C. *J. Med. Chem.* **2002**, *45*, 2994.
8. Pevarello, P.; Brasca, M. G.; Amici, R.; Orsini, P.; Traquandi, G.; Corti, L.; Piutti, C.; Sansonna, P.; Villa, M.; Pierce, B. S.; Pulici, M.; Giordano, P.; Martina, K.; Fritzen, E. L.; Nugent, R. A.; Casale, E.; Cameron, A.; Ciomei, M.; Roletto, F.; Isacchi, A.; Fogliatto, G.; Pesenti, E.; Pastori, W.; Marsiglio, A.; Leach, K. L.; Clare, P. M.; Fiorentini, F.; Varasi, M.; Vulpetti, A.; Warpehoski, M. A. *J. Med. Chem.* **2004**, *47*, 3367.
9. Manfredini, S.; Bazzanini, R.; Baraldi, P. G.; Guarneri, M.; Simoni, D.; Marongiu, M. E.; Pani, A.; Tramontano, E.; La Colla, P. *J. Med. Chem.* **1992**, *35*, 917.
10. Park, H.-A.; Lee, K.; Park, S.-J.; Ahn, B.; Lee, J.-C.; Cho, H. Y.; Lee, K.-I. *Bioorg. Med. Chem. Lett.* **2005**, *15*, 3307.
11. Tanitame, A.; Oyamada, Y.; Ofuji, K.; Fujimoto, M.; Iwai, N.; Hiyama, Y.; Suzuki, K.; Ito, H.; Wachi, M.; Yamagishi, J. *J. Med. Chem.* **2004**, *47*, 3693.
12. Genin, M. J.; Allwine, D. A.; Anderson, D. J.; Barbachyn, M. R.; Emmert, D. E.; Garmon, S. A.; Graber, D. R.; Grega, K. C.; Hester, J. B.; Hutchinson, D. K.; Morris, J.; Reischer, R. J.; Ford, C. W.; Zurenko, G. E.; Hamel, J. C.; Schaadt, R. D.; Stapert, D.; Yagi, B. H. *J. Med. Chem.* **2000**, *43*, 953.
13. Bekhit, A. A.; Fahmy, H. T. Y.; Rostom, S. A. F.; Baraka, A. M. *Eur. J. Med. Chem.* **2003**, *38*, 27.
14. Menozzi, G.; Mosti, L.; Fossa, P.; Mattioli, F.; Ghia, M. *J. Heterocycl. Chem.* **1997**, *34*, 963.
15. Sridhar, R.; Perumal, P. T.; Etti, S.; Shanmugam, G.; Ponnuswamy, M. N.; Prabavathy, V. R.; Mathivanan, N. *Bioorg. Med. Chem. Lett.* **2004**, *14*, 6035.
16. Kees, K. L.; Fitzgerald, J. J.; Steiner, K. E.; Mattes, J. F.; Mihan, B.; Tosi, T.; Mondoro, D.; McCaleb, M. L. *J. Med. Chem.* **1996**, *39*, 3920.
17. Bebermiz, G. R.; Argentieri, G.; Battle, B.; Brennan, C.; Balkan, B.; Burkey, B. F.; Eckhardt, M.; Gao, J.; Kapa, P.; Strohschein, R. J.; Schuster, H. F.; Wilson, M.; Xu, D. *J. Med. Chem.* **2001**, *44*, 2601.
18. Genin, M. J.; Biles, C.; Keiser, B. J.; Poppe, S. M.; Swaney, S. M.; Tarpley, W. G.; Yagi, Y.; Romero, D. L. *J. Med. Chem.* **2000**, *43*, 1034.
19. Hashimoto, H.; Imamura, K.; Haruta, J.-I.; Wakitani, K. *J. Med. Chem.* **2002**, *45*, 1511.
20. Habeeb, A. G.; Rao, P. N. P.; Knaus, E. E. *J. Med. Chem.* **2001**, *44*, 3039.
21. Sakya, S. M.; DeMello, K. M. L.; Minich, M. L.; Rast, B.; Shavnya, A.; Rafka, R. J.; Koss, D. A.; Cheng, H.; Li, J.; Jaynes, B. H.; Ziegler, C. B.; Mann, D. W.; Petras, C. F.; Seibel, S. B.; Silvia, A. M.; George, D. M.; Lund, L. A.; St. Denis, S.; Hickman, A.; Michelle, L.; Haven, M. L.; Lynch, M. P. *Bioorg. Med. Chem. Lett.* **2006**, *16*, 288.
22. Čaleta, I.; Kralj, M.; Marjanović, M.; Bertoša, B.; Tomić, S.; Pavlović, G.; Pavelić, K.; Karminski-Zamola, G. *J. Med. Chem.* **2009**, *52*, 1744.
23. Bertoša, B.; Kojić-Prodić, B.; Ramek, M.; Piperaki, S.; Tsantili-Kakoulidou, A.; Wade, R.; Tomić, S. *J. Chem. Inf. Model.* **2003**, *43*, 1532.
24. Bertoša, B.; Aleksić, M.; Karminski-Zamola, G.; Tomić, S. *Int. J. Pharm.* **2010**, *394*, 106.
25. Wei, F.; Zhao, B.-X.; Huang, B.; Zhang, L.; Sun, C.-H.; Dong, W.-L.; Shin, D.-S.; Miao, J.-Y. *Bioorg. Med. Chem. Lett.* **2006**, *16*, 6342.
26. Xia, Y.; Dong, Z.-W.; Zhao, B.-X.; Ge, X.; Meng, N.; Shin, D.-S.; Miao, J.-Y. *Bioorg. Med. Chem.* **2007**, *15*, 6893.
27. Xia, Y.; Fan, C.-D.; Zhao, B.-X.; Zhao, J.; Shin, D.-S.; Miao, J.-Y. *Eur. J. Med. Chem.* **2008**, *43*, 2347.
28. Fan, C.-D.; Zhao, B.-X.; Wei, F.; Zhang, G.-H.; Dong, W.-L.; Miao, J.-Y. *Bioorg. Med. Chem. Lett.* **2008**, *18*, 3860.
29. Ding, X.-L.; Zhang, H.-Y.; Oi, L.; Zhao, B.-X.; Lian, S.; Lv, H.-S.; Miao, J.-Y. *Bioorg. Med. Chem. Lett.* **2009**, *19*, 5325.
30. Zheng, L.-W.; Wu, L.-L.; Zhao, B.-X.; Dong, W.-L.; Miao, J.-Y. *Bioorg. Med. Chem. Lett.* **1957**, 2009, 17.
31. Fortuna, C. G.; Barresi, V.; Berellini, G.; Musumarra, G. *Bioorg. Med. Chem.* **2008**, *16*, 4150.
32. Cruciani, G.; Crivori, P.; Carrupt, P.-A.; Testa, B. *J. Mol. Struct.: THEOCHEM.* **2000**, *503*, 17.
33. Cruciani, G.; Pastor, M.; Guba, W. *Eur. J. Pharm. Sci.* **2000**, *11*, S29.
34. Madonna, S.; Beclin, C.; Laras, Y.; Moret, V.; Marcowycz, A.; Lamoral-Theys, D.; Dubois, J.; Barthelemy-Requin, M.; Lenglet, G.; Depauw, S.; Cresteil, T.; Aubert, G.; Monnier, V.; Kiss, R.; David-Cordonnier, M.-H.; Kraus, J.-L. *Eur. J. Med. Chem.* **2010**, *45*, 623.
35. Eloy, F.; Lenaers, R. *Chem. Rev.* **1962**, *62*, 155.
36. Pearse, G. A., Jr.; Pflaum, R. T. *J. Am. Chem. Soc.* **1959**, *81*, 6505.
37. Malca-Mor, L.; Stark, A.-A. *Appl. Environ. Microbiol.* **1982**, *44*, 801.
38. Brooks, D. G.; James, R. M.; Patek, C. E.; Williamson, J.; Arends, M. *J. Oncogene* **2001**, *20*, 2144.
39. Cory, A. H.; Owen, T. C.; Barltrop, J. A.; Cory, J. G. *Cancer Comm.* **1991**, *3*, 207.
40. Müller, K.; Faeh, C.; Diedrich, F. *Science* **1881**, 2007, 317.
41. Goodford, P. J. *J. Med. Chem.* **1985**, *28*, 849.
42. Huang, X.-M.; Xiao, J.-H.; Li, J.-T.; Zhang, Z.-Q.; Ruan, J.-X. *Int. J. Pharm.* **2006**, *309*, 109.
43. Tomić, S.; Bertoša, B.; Wang, T.; Wade, R. C. *Proteins: Struct. Funct. Bioinf.* **2007**, *67*(2), 435.